

# Permeability and Metabolic Properties of a Trophoblast Cell Line (*HRP-1*) Derived from Normal Rat Placenta

Fenglin Shi, Michael J. Soares,\* Michael Avery, Fei Liu, Xiaoman Zhang, and Kenneth L. Audus<sup>1</sup>

*Department of Pharmaceutical Chemistry, The University of Kansas, Lawrence, Kansas 66047; and*

*\*Department of Physiology, The University of Kansas Medical Center, Kansas City, Kansas 66160*

**The *HRP-1* cell line is derived from normal rat placenta and appears morphologically similar to and retains characteristic expression of cellular markers of labyrinthine trophoblast cells. In this study, monolayers of *HRP-1* cells grown on permeable supports were evaluated as a potential *in vitro* system to study trophoblast transport and metabolism. The cell line was shown to express and retain functional activity of the predominant placental cytochrome P450 isozyme, CYP1A1. Additionally, the *HRP-1* cells retain functional activity of angiotensin I converting enzyme and carboxypeptidase N-like enzyme, peptidases characteristic of the trophoblast. The permeation of several hydrophilic, inert markers across the *HRP-1* monolayers was observed to be dependent on effective molecular size and to be passive in nature. Functional asymmetry of the *HRP-1* cells was illustrated by the predominant permeation of linoleic acid in the apical-to-basolateral direction across the monolayers. Transferrin passage across *HRP-1* monolayers was concentration-dependent, was bidirectional, and could be inhibited by unlabeled transferrin, features typical of the trophoblast transport system for transferrin. Collectively, these properties suggest that the *HRP-1* cell line may provide a useful tool for evaluating some of the permeability and metabolic properties of the trophoblast.** © 1997 Academic Press

## INTRODUCTION

The placenta serves as a mediator between the maternal and fetal circulations, providing for nutrient and waste transport, gas exchange, and hormone production [1]. The mammalian chorioallantoic placenta differs among species and is classified based on the tissue layers intervening between the maternal and the fetal circulations. The laboratory rat placenta has three trophoblast layers and is classified as hemotrichorial. The human placenta, having only one layer, is classified as

hemomonochorial [2]. The three trophoblast layers of the labyrinth zone of the rat chorioallantoic placenta appear to be the rate-limiting permeability barrier to the exchanges of substances between maternal and fetal compartments [3]. The labyrinth zone, in order from the maternal blood sinus inward to the fetal capillary, consists of an initial trophoblast layer (layer I) composed of mononucleated cells in direct contact with the maternal blood. The second and third trophoblast layers (layers II and III, respectively) are both syncytial. Only layer I and the fetal capillary endothelium are permeable to lanthanum and horseradish peroxidase [4–6]. Therefore, within the rat placenta, layers II and III are considered to be the rate-limiting permeability barriers [3].

A single syncytiotrophoblast forms the rate-limiting permeability barrier in the human placenta. The enzyme alkaline phosphatase is predominantly localized to the maternal-facing syncytial plasma membrane of this rate-limiting permeability barrier. This is noteworthy in that, in the rat placenta, alkaline phosphatase is also localized to the maternal-facing plasma membrane of layer II trophoblasts [7, 8]. Similarly, in the mouse, alkaline phosphatase is present in the trophoblast layer constituting the rate-limiting permeability barrier [9]. These observations indicate that alkaline phosphatase seems to be co-localized with the trophoblast layer forming the rate-limiting permeability barrier of the placenta of rat, human, and mouse [3, 7–9] and could be a marker for trophoblasts responsible for determining some of the permeability properties of the placenta.

Cell lines such as *HRP-1* have been derived from the labyrinth zone of the normal rat placenta. The *HRP-1* cells appear morphologically similar to labyrinthine trophoblast cells [10, 11] and retain expression of alkaline phosphatase [12, 13], cytokeratins [13], and transferrin receptors [13, 14], additional markers for labyrinthine trophoblasts. The *HRP-1* cell line is a trophoendodermal stem cell population that arises after midgestation with the capability of differentiating into cells resembling trophoblast and yolk sac phenotypes. Harvested from the midgestation chorioallantoic pla-

<sup>1</sup> To whom reprint requests should be addressed. Fax: (913) 864-5736. E-mail: audus@smisson.hbc.ukans.edu.

centa, *HRP-1* cells are readily adaptable to propagation both *in vitro* and *in vivo* [12, 14]. The purpose of this study was to evaluate the suitability of subcultures of *HRP-1* cells for investigation of trophoblast transport and metabolism *in vitro*. Unlike most trophoblast cultures, the *HRP-1* cells grow to form confluent monolayers which can facilitate trans-trophoblast transport experiments. Furthermore, the appearance of alkaline phosphatase in the *HRP-1* cells, an enzyme coincident in trophoblasts that provide the rate-limiting permeability properties of the placenta *in vivo*, prompted consideration of the cell line's potential utility in studying trophoblast transport and metabolism.

## MATERIALS AND METHODS

Transferrin (human) fluorescein conjugate, 7-ethoxyresorufin, and resorufin were purchased from Molecular Probes (Junction City, OR). Tissue culture medium, antibiotics,  $\beta$ -glucuronidase/arylsulfatase, DMSO, fluorescein, fluorescein isothiocyanate-conjugated dextrans, anti-mouse IgG (Fab) peroxidase conjugate, and angiotensin I converting enzyme assay kit were purchased from Sigma Chemical Co. (St. Louis, MO). Monoclonal antibody, CYP1A1, and induced liver samples were purchased from Xenotech (Kansas City, KS). Hyperfilm-ECL was purchased from Amersham (Arlington Heights, IL). ScintiVerse BD was purchased from Fisher Scientific (Fair Lawn, NJ).  $\beta$ -Mercaptoethanol was purchased from Bio-Rad Laboratories (Hercules, CA). Heat-inactivated fetal bovine serum was purchased from JRH Biosciences (Lenexa, KS). [ $^{14}$ C]Sucrose and [ $^{14}$ C]urea were purchased from ICN Biomedicals, Inc. (Irvine, CA). [ $^3$ H]Mannitol and [ $^3$ H]methotrexate were purchased from DuPont NEN Research Products (Boston, MA). [ $^{14}$ C]Linoleic acid was purchased from Amersham Life Sciences Co. (Little, CA). Protein assay kits (BCA Protein Assay with bovine serum standards) were purchased from Pierce Science and Analytical Research Products (Rockford, IL). All other reagents were of the highest grade commercially available.

**Culture of *HRP-1* cells.** *HRP-1* cells [11, 12] were maintained in culture medium containing RPMI 1640, NaHCO<sub>3</sub>, pH 7.4, 1 mM sodium pyruvate, 50  $\mu$ M  $\beta$ -mercaptoethanol, 100 units/ml penicillin, 100  $\mu$ g/ml streptomycin, and 5–10% heat-inactivated fetal bovine serum. The cells were seeded in 75- or 175-cm<sup>2</sup> flask and incubated at 37°C with 5% CO<sub>2</sub> [12]. The cells were fed every other day. The *HRP-1* cells were harvested for passaging after 3 to 4 days by trypsin-EDTA (0.25% trypsin and 0.02% EDTA in Hanks' balanced salt solution) treatment. Cells from passages 12–16 were used for all of the studies described herein.

**Microsome preparation.** *HRP-1* cells were grown in 175-cm<sup>2</sup> flasks to confluent monolayers. The *HRP-1* cells were washed with ice-cold phosphate-buffered saline (PBS), pH 7.4. The cells were then bathed in a buffer containing 50 mM Tris-HCl, pH 7.4, 150 mM KCl, and 2 mM EDTA. The cells were scraped from the flask and centrifuged at 1000g for 10 min. The cell pellet was then resuspended in buffer containing 0.25 M sucrose in 50 mM Tris-HCl, pH 7.4. Sonication of the suspension for 1–2 min produced a suspension of cytosolic and nuclear proteins. To remove mitochondrial proteins from suspended membrane fragments, cell fractions were centrifuged at 10,000g for 15 min. The supernatant was centrifuged at 100,000g for 1 h at 10°C. The microsomal pellet was resuspended in 0.25 M sucrose and the protein concentration determined by BCA. All microsomal preparations were stored at -70°C.

**Immunoblots.** Microsome preparations (0.5 to 10  $\mu$ g *HRP-1* protein and 0.05  $\mu$ g induced rat liver protein) were subjected to SDS-PAGE, 12% acrylamide Tris-glycine [15]. All microsomal samples were heated to 100°C for 10 min and then centrifuged at 10,000g for

5 min. Molecular weight markers (4 to 250 kDa) and purified bovine serum albumin (0.5  $\mu$ g) served as controls. Electrophoresis of microsomes with SDS-PAGE was monitored at 95 V for 2.5 h. Following electrophoresis, protein was either transferred electrophoretically to PVDF or polyacrylamide gels and then exposed to Coomassie blue stain (0.1% Coomassie blue, 45% methanol, 2% acetic acid) for 1 h. Destaining polyacrylamide not used in electrophoretic transfer of microsomal protein required destaining overnight to visualize the protein bands. No proteins greater than 69 kDa were detected.

Following SDS-PAGE, microsomal proteins were transferred electrophoretically to PVDF membrane (45 V, 2 h). After electrophoresis transfer, PVDF membranes were immersed in Ponceau S staining solution for 5 min to verify the presence of microsomal protein. The Ponceau S stain was removed in an aqueous solution containing 10% acetic acid (v/v) for approximately 4–5 min. To block nonspecific binding with the monoclonal antibody, membranes were incubated for 2 h with PBS, pH 7.4, containing 10% dry milk (w/v), 2% bovine serum albumin (w/v), and 0.1% Tween 20. The membranes were then incubated with monoclonal antibody CYP1A1 (10  $\mu$ g/ml) or a preimmune mouse antibody (nonspecific IgG, 10  $\mu$ g/ml) in 10 mM Tris-HCl, pH 7.4, containing 0.1% Tween 20. All microsomal protein bound to PVDF membranes was incubated overnight at room temperature with the monoclonal antibody or the nonspecific IgG. A secondary antibody, IgG peroxidase conjugate specific for the CYP1A1 monoclonal antibody, was diluted 1:80,000 in 10 mM Tris-HCl containing 0.05% Tween 20 and incubated with the PVDF membrane for 1 h at 25°C. CYP1A1 was detected by enhanced chemiluminescence by incubating PVDF immunoblots at 25°C for 45 s and then exposing them to Hyperfilm-ECL.

**Activity assays for cytochrome P450.** Microsomal cytochrome P450 1A (CYP 1A1) activity was measured fluorometrically by the O-dealkylation of 7-ethoxyresorufin producing resorufin according to Dutton and Parkinson [16] with minor modifications according to Shiverick *et al.* [17]. Reaction mixtures of 1 ml final volume were incubated at 37°C. The reaction mixture contained potassium phosphate buffer (100 mM, pH 7.4), MgCl<sub>2</sub> (3 mM), EDTA (1 mM), NADP (1 mM), glucose 6-phosphate (5 mM), glucose-6-phosphate dehydrogenase (1 unit/ml), and 7-ethoxyresorufin (10  $\mu$ M). Blanks did not contain NADP. Reactions were started by the addition of the NADPH-generating system and stopped after 8 min with 2 ml of ice-cold acetone. Protein was removed by centrifugation at 1000g for 10 min and the supernatant was transferred to clean quartz cuvettes. Fluorescence was measured at an emission of 585 nm and an excitation wavelength of 535 nm in an SLM Aminco 4800 spectrofluorometer.

The method of Donato *et al.* [18] was used to assay CYP1A1 in intact cell cultures. *HRP-1* cells were grown in 6-well culture dishes and 7-ethoxyresorufin and dicumarol were added to the cells. Following addition of  $\beta$ -glucuronidase/arylsulfatase in 0.1 M sodium acetate, the cell supernatants were further incubated for 2 h at 37°C. The amount of resorufin was measured with excitation of 530 nm and emission of 590 nm.

**Angiotensin converting enzyme and carboxypeptidase N-like activity.** To assay both angiotensin converting enzyme and carboxypeptidase N-like enzyme activities, *HRP-1* cells were grown to confluent monolayers in 175-cm<sup>2</sup> flasks.

For angiotensin converting enzyme, homogenates were prepared according to Shi and Audus [19]. Briefly, the tissues were homogenized in 0.25 M sucrose and frozen on dry ice and thawed, six times. The homogenates were centrifuged at 15,000g for 5 min and the supernatant was saved at -70°C until assayed. Angiotensin converting enzyme activity in the supernatants was assayed with a Sigma Chemical Co. 305-UV kit. Absorbance of the samples was measured at 340 nm with a Shimadzu UV-visible spectrophotometer. Blanks contained boiled supernatant.

Carboxypeptidase N-like enzyme activity in the *HRP-1* cells was assayed according to the method of Skidgel and Erdos [20]. Briefly,

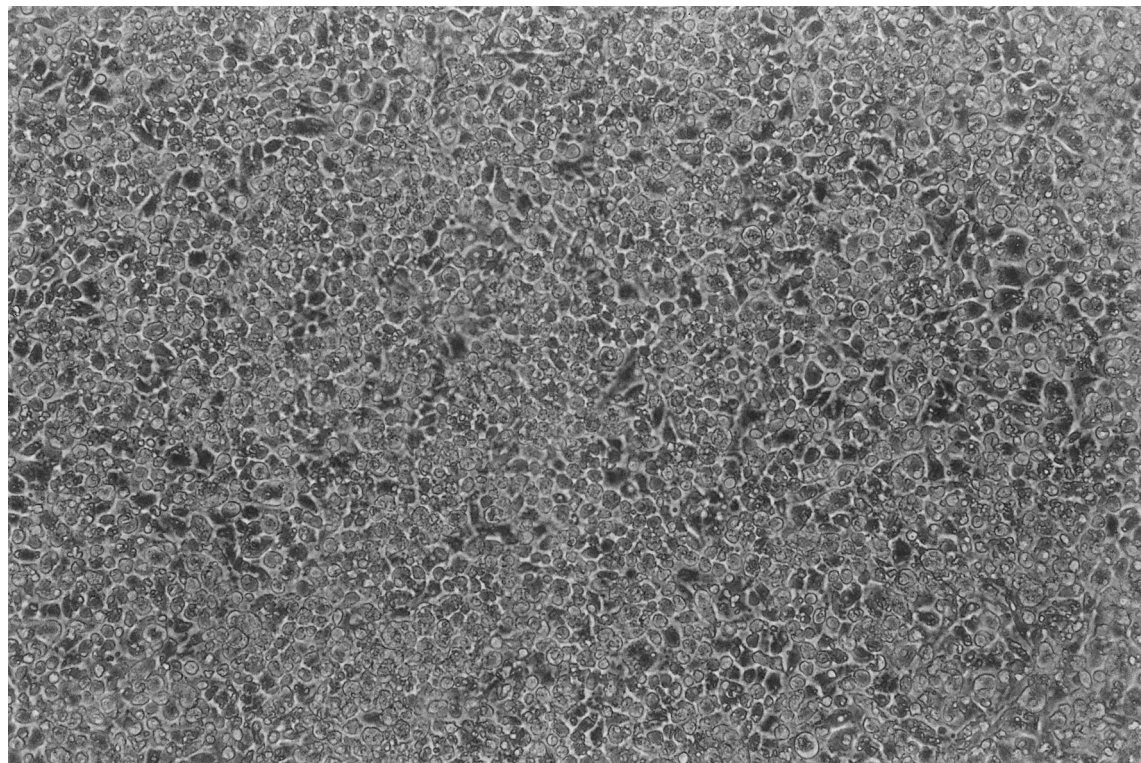


**FIG. 1.** Light photomicrograph of *HRP-1* cells after 5 days in culture. Magnification 100 $\times$ .

the cells were collected by scraping from the flasks, broken up by sonication, and centrifuged at 1300*g* for 5 min. A sample of the supernatant was mixed in a 0.25 *M* Tris buffer, pH 7.5, containing 10 *mM*  $\text{CoCl}_2$  in a total volume of 0.2 ml, and incubated for 2 h at 4°C. The solution was made 5 *mM* in Bz-Gly-Lys (hippuryl-Lys) by addition of 0.05 ml of stock and the incubation continued for an additional 3 h at 37°C. After the incubation period, 0.25 ml of 1 *M* HCl was added to the solution followed by 1.5 ml of ethyl acetate. The samples were vortexed and centrifuged at 500*g* for 5 min. The top organic layer was transferred to appropriate tubes and evaporated at 120°C. The tubes received 1 ml of water and were vortexed, and the absorbance was then measured at 228 nm in a Shimadzu UV-visible spectrophotometer against a blank prepared from boiled supernatant.

**Transmonolayer permeability.** *HRP-1* cells ( $1 \times 10^7$ ) were grown onto rat-tail-collagen-coated polycarbonate membranes placed on the growth surface of 100-mm tissue culture dishes. Cells were fed with *HRP-1* cell culture medium containing RPMI 1640,  $\text{NaHCO}_3$ , HEPES, pyruvic acid,  $\beta$ -mercaptoethanol, antibiotics, and heat-inactivated fetal bovine serum. Cells were grown to monolayers in 5–7 days. The 13-mm, 3- $\mu\text{m}$ -pore polycarbonate membranes with cell monolayers grown on their surfaces were placed between side-by-side diffusion cells (Crown Glass Co., Somerset, NJ) for permeability studies [19]. Both the donor chamber and the receiver chamber were filled with 3.0 ml of PBSA buffer containing 129 *mM* NaCl, 2.5 *mM* KCl, 7.4 *mM*  $\text{Na}_2\text{HPO}_4$ , 1.3 *mM*  $\text{KH}_2\text{PO}_4$ , 0.63 *mM*  $\text{CaCl}_2$ , 0.74 *mM*  $\text{MgSO}_4$ , 5.3 *mM* glucose, pH 7.4. The *HRP-1* cell monolayers were oriented in the diffusion apparatus so that the cells faced the donor chamber (apical side) and the polycarbonate membrane faced the receiver chamber (basolateral side). Polycarbonate membranes treated with rat-tail collagen but without cell monolayers were used as controls. The diameter of the diffusion area was 9 mm. The water jacket surrounding the donor and the receiver chambers was constantly thermostated

at 37°C. The contents of each chamber were continuously stirred at 600 rpm with magnetic stir bars. Either fluorescein-conjugated dextrans or radioisotope-labeled compounds with different concentrations or different molecular weights were pulsed into the donor chambers. A 0.2-ml aliquot from the receiver chamber was taken at several time points up to 70 min. An SLM AMINCO Subnanosecond Life-time Fluorometer (Urbana, IL) was used to assay the fluorescein in the samples in microcuvettes following dilution with 1.8 ml of PBSA [19]. The wavelength of excitation was 490 nm and emission was monitored at 520 nm. The samples of radioisotope-labeled compounds were placed in scintillation vials and diluted with 10 ml of ScintiVerse BD. Samples were counted in a LS 7500 Beckman scintillation counter.

**Statistics.** All experiments were carried out in at least triplicate or quadruplicate samples and the data are expressed in the figures or text as the mean  $\pm$  standard deviation (SD). The number, *n*, in the figure legends indicates the number of replicates from different *HRP-1* monolayers. Data were normalized for the total milligrams of cell protein per sample, determined with a BCA Protein Assay.

Apparent permeability coefficients were calculated using the formula:  $P = X/(A \times t \times C_d)$ , where *P* is the apparent permeability coefficient (cm/s), *X* is the amount of substance (mol) in the receptor chamber at time *t* (s), *A* is the diffusion area (0.636  $\text{cm}^2$ ), and *C<sub>d</sub>* is the concentration of the substance in the donor chamber (mol/ $\text{cm}^3$ ). The flux (mol/cm/s) of a substance across the *HRP-1* cell monolayers was calculated at the linearly regressed slope through linear data (e.g., sampling times, 1–70 min) [19, 21].

The apparent permeability of the *HRP-1* monolayers, *P<sub>e</sub>*, was calculated by the relationship  $1/P = 1/P_e + 1/P_c$ , where *P<sub>c</sub>* is the apparent permeability coefficient of collagen-coated polycarbonate membranes in the absence of cells [21].



**FIG. 2.** Light photomicrograph of a cross section of *HRP-1* cells grown on polycarbonate membranes. Cells were stained with hematoxylin and eosin and observed at a magnification of 400 $\times$ .

## RESULTS

*HRP-1* cells grow rapidly and form monolayers of flattened polygonal-shaped cells on rat-tail-collagen-coated surfaces, including polycarbonate membranes or plastic culture dishes. A typical 5-day-old subculture of *HRP-1* cell monolayers grown on a plastic culture dish is shown in Fig. 1. Cross sections of *HRP-1* cells grown on polycarbonate membranes were used to verify the presence of a single layer of cells. Figure 2 shows a representative example of *HRP-1* cells grown on the polycarbonate support after 5 days in culture.

A Western blot of microsomal protein from the *HRP-1*, shown in Fig. 3, indicated the expression of small amounts of the cytochrome P450 isozyme CYP1A1 in the cells. The cell proteins were run against a positive control, the induced rat liver sample, and a negative control, bovine serum albumin (not shown). The monoclonal antibody specifically recognizes the CYP1A1 protein (upper band) and also cross-reacts with the induced form of the isozyme, CYP1A2 (lower band), in the *HRP-1* and liver samples but not in the negative control, bovine serum albumin. The cross-reactivity was particularly obvious in the induced rat liver sample. Minor immunoreactivity for CYP1A2 also appeared in the *HRP-1* cells as shown in Fig. 3. Similar

blots using the nonspecific mouse IgG revealed no immunoreactivity (not shown).

The level of 7-ethoxyresorufin *O*-deethylase (EROD) activity, a functional marker for CYP1A1, was low but consistent in both *HRP-1* microsomes and intact *HRP-1* cells as summarized in Fig. 4. The EROD activity was essentially constant over a period of 2 to 12 days in microsomes prepared from cultures and in the intact cell cultures. Two additional enzymes were chosen for assay in the *HRP-1* cell line as part of the functional

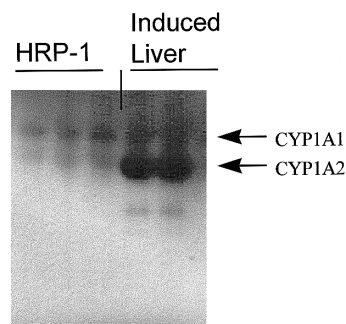


**FIG. 3.** Western blot of microsomal protein from confluent *HRP-1* cell monolayers and microsomal protein from induced rat liver. The monoclonal antibody recognizes cytochrome P450 isozyme CYP1A1 and reacts with CYP1A2.

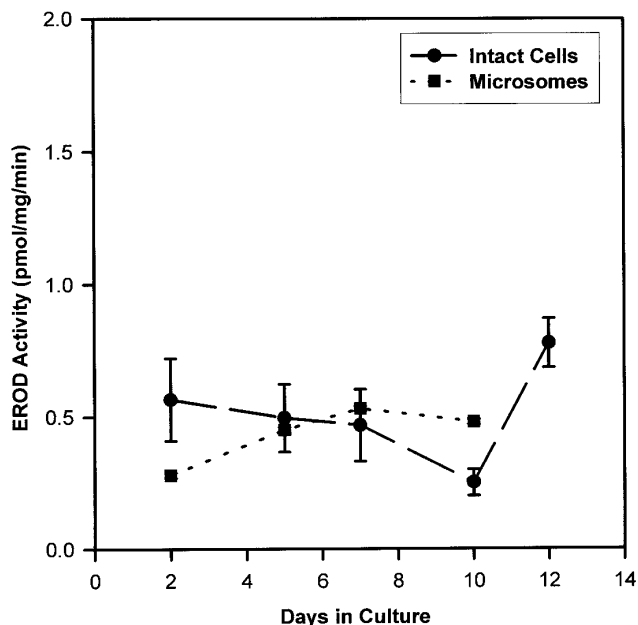


FIG. 4. 7-Ethoxyresorufin *O*-deethylase (EROD) activity in microsomes and in intact *HRP-1* cell monolayers ( $n = 4$ ).

enzymatic characterization of the cells. Substantial levels of activity for both angiotensin converting enzyme,  $1.0 \pm 0.1$  nmol/mg/min, and carboxypeptidase N-like enzyme,  $0.6 \pm 0.1$   $\mu$ mol/mg/min, were found in homogenates prepared from *HRP-1* cells after 5 days in culture.

The permeation of selected hydrophilic, paracellular markers (e.g., mannitol, sucrose, fluorescein, and fluorescein conjugated dextrans with average molecular weights of 4400 to 147,800) across monolayers of *HRP-1* cells, shown in Fig. 5, indicated a sieving effect based on effective molecular size. The passage of the markers across polycarbonate membranes alone was substantially greater than with *HRP-1* monolayers present and was used to calculate the apparent permeability coefficients for the cells ( $P_e$ ) shown in Fig. 5. The application of regressed lines through the data indicated that there was one series of markers, with molecular weights of 182 to about 4400 (i.e., an effective molecular radii of  $<12$  Å), in which the *HRP-1* monolayer permeability was linear ( $r^2 = 0.90$ ) but rather insensitive to molecular weight (i.e., shallow slope). For the other series of markers with molecular weights above about 4400 (i.e., effective molecular radii  $>12$  Å), the permeability drops linearly ( $r^2 = 0.94$ ) and was highly dependent on molecular weight (i.e., steep slope).

Urea and methotrexate, also included in Fig. 5, were representative of small hydrophilic molecules that may interact with tissue barriers, in addition to undergoing diffusion through the paracellular pathway. Urea was used as an example of an agent that crosses cell sys-

tems both transcellularly and paracellularly and had a permeability much greater than any of the purely paracellular markers. Methotrexate, on the other hand, was example of an agent that undergoes extensive binding and uptake by trophoblasts and, consequently, had a much lower permeability than might be predicted by the molecular weight.

The difference between the apical-to-basolateral and the basolateral-to-apical permeation of linoleic acid across *HRP-1* monolayers was used to assess the functional asymmetry of the cells. Linoleic acid was mixed with bovine serum albumin in a ratio of 6:1 (fatty acid:albumin), and the permeation of the fatty acid was monitored in both directions across collagen-coated polycarbonate membranes alone and in the presence of *HRP-1* monolayers. Figure 6 summarizes data that indicated a predominant apical-to-basolateral permeation of linoleic acid across *HRP-1* monolayers. By contrast, passage of linoleic acid across collagen-coated polycarbonate membranes in the absence of cells was not asymmetric and substantially greater. The passage of the fatty acid across the *HRP-1* monolayers was sensitive to reduced temperature and suggested a cell-mediated permeation pathway.

Transferrin was examined as a representative large molecule that crosses tissue barriers by mechanisms alternative to paracellular routes. Transferrin, at 75 nM, had an apparent permeability coefficient of  $3.5 \pm 0.2 \times 10^{-5}$  cm/s or significantly higher than apparent permeabilities observed for the paracellular marker dextrans of similar molecular weight. Figure 7 shows

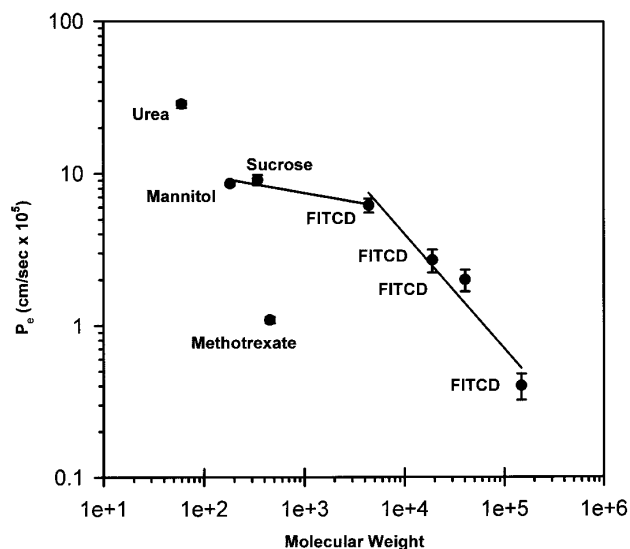
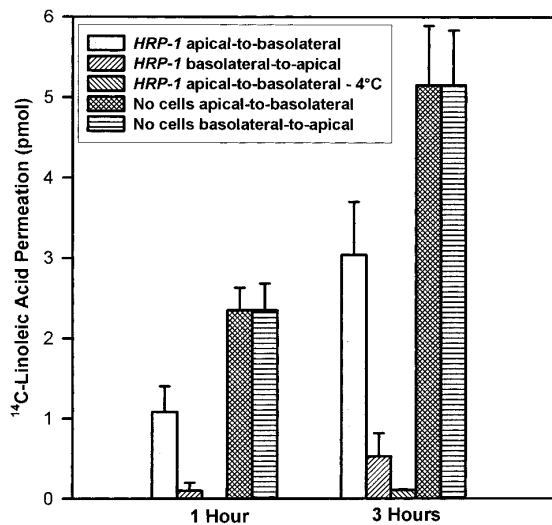
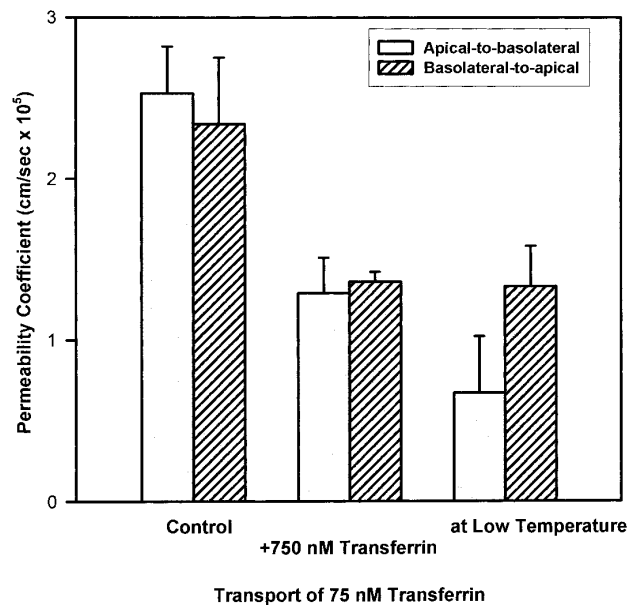


FIG. 5. The dependence of apparent permeability coefficient ( $P_e$ ) for the passage of selected substances across *HRP-1* cell monolayers on molecular weight at 37°C ( $n = 4$ ).  $P_e$  was calculated as described under Materials and Methods. FITCD, fluorescein isothiocyanate-conjugated dextran.



**FIG. 6.** Bidirectional permeation of [ $^{14}\text{C}$ ]inoleic acid across *HRP-1* monolayers and collagen-coated polycarbonate membranes ( $n = 4$ ). Except for the indicated bar all data were collected from experiments performed at  $37^\circ\text{C}$ .

that the passage of transferrin across *HRP-1* cell monolayers was concentration-dependent and was saturable at higher concentrations. The half-maximal concentration of the saturable transport was about  $60\text{ nM}$  (estimated with Sigma Plot, version 2.0). In addition, the permeation rate of transferrin across the monolayers was bidirectional with the trend of apical-to-basolateral permeation being only slightly greater than the permeation rate of the protein in the basolateral-to-apical direction. The passage of transferrin across the



**FIG. 8.** Apparent permeability coefficients for the bidirectional passage of  $75\text{ nM}$  transferrin across *HRP-1* monolayers in the absence of any treatment (Control), or the presence of a 10-fold excess of unlabeled transferrin ( $+750\text{ nM}$  Transferrin), or at  $4^\circ\text{C}$  (Low Temperature) ( $n = 4$ ).

*HRP-1* monolayers was inhibited by an excess amount of unlabeled transferrin and by low temperatures, as illustrated in Fig. 8, an additional indication of the involvement of a transcytotic mechanism.

## DISCUSSION

*HRP-1* is a well-studied normal rat cell line that has proven useful for identifying factors controlling trophoblast growth and differentiation. Particularly notable is the rapid and convenient growth of *HRP-1* cells and their retention of morphological and biochemical features consistent with normal trophoblasts of the labyrinth zone [11, 12], including the presence of a typical nutrient transporter [22]. Perhaps more importantly, the *HRP-1* cell line has the ability to form monolayers, a property that permits evaluation of transcellular transport and access to apical and basolateral surfaces of the monolayer. By contrast, primary cultures of human cytotrophoblasts form a syncytium that does not completely cover a growth surface [23] and does not permit trans-trophoblast transport studies. This normal cell line could also potentially provide a convenient and more easily manipulated corollary to rat studies *in vivo*. The purpose of our study was to initiate an evaluation of the applicability of the *HRP-1* monolayers for mechanistic studies of trans-trophoblast transport and metabolism of therapeutic agents and drugs of abuse *in vitro*.

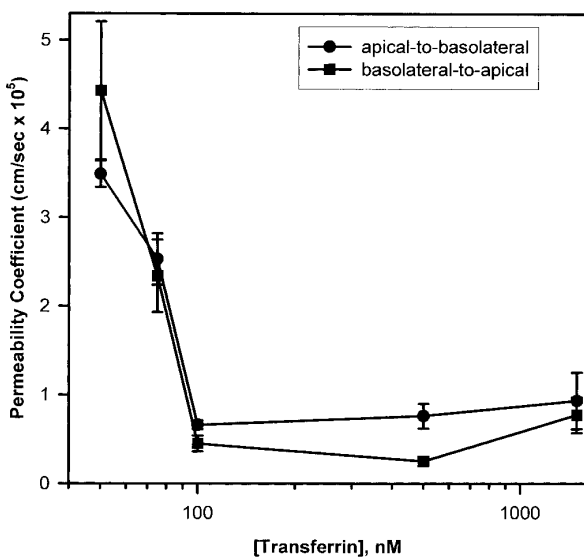


**FIG. 7.** Apparent permeability coefficients for the bidirectional passage of transferrin across *HRP-1* monolayers at  $37^\circ\text{C}$  ( $n = 4$ ).

Several drugs of abuse and other xenobiotics undergo oxidative metabolism in the human placenta. The placenta has at least one constitutive and one induced form of the cytochrome P450 isozyme, CYP1A1, which is localized in the trophoblast [24]. Expression and retention of CYP1A1 activity then will be a required marker for any cell culture system proposed for studying placental drug metabolism. The *HRP-1* cell line retains low levels of CYP1A1 relative to the induced rat liver and as documented by Western blots and measured by EROD activity. The low EROD activity in the *HRP-1* monolayers was in good agreement with the literature on rat [17] and human placenta [24, 25], both of which retain very low constitutive levels of CYP1A1 relative to the liver. As examples, in the nonsmoking human placental microsome, the EROD activity was reported to be in the range of 0.20 to 0.35 pmol/mg/min [25] and in rat labyrinth zone microsomes, <1 pmol/mg/min [17]. Our immunoblots also confirmed indications of the induced CYP1A1 form, CYP1A2, in the *HRP-1* cells. In the rat and human, induction of CYP1A2 in the placenta occurs through exposure to polycyclic hydrocarbons [17, 24].

The plasma membrane of the syncytiotrophoblast facing the maternal blood has been found to be rich in certain peptidases that may regulate the passage of peptides across the placental barrier. In particular, microvillar membranes from human syncytiotrophoblasts were observed to be enriched in angiotensin I converting enzyme, angiotensinase A, carboxypeptidase N-like enzyme, and neutral endopeptidase ("Enkephalinase") [26]. On that basis, we elected to determine whether two of the peptidases, angiotensin I converting enzyme and carboxypeptidase N-like enzyme, were retained in the *HRP-1* system. The presence of significant activity of both enzymes was observed in the *HRP-1* cells. Relative to one of the few available reports on peptidase activity in the placenta [26], our observations suggest the cell line may be useful in examining trophoblast metabolism of some peptides. In ongoing studies, this *in vitro* system is being used to examine the metabolic fate of both drugs of abuse and opioid peptides in order to validate the utility of the system in evaluating trophoblast metabolism.

Passive diffusion is the primary mechanism by which xenobiotics cross the placental barrier [3, 27–30]. An appropriate *in vitro* system might be expected to provide at least a qualitative representation of the sieving of molecules observed in the placenta. The passive permeation of selected hydrophilic markers across the *HRP-1* monolayers was found to be linearly related to molecular size. The  $P_e$  was also proportional to the water diffusion coefficients for the markers (not shown), consistent with the trans-trophoblast passage of small hydrophilic solutes in the placenta [27–30]. Faber [27], for example, previously demonstrated that, excluding

urea, small-molecular-radius (<10-Å) markers (e.g., mannitol, sucrose, and fluorescein-conjugated dextran, MW 4000) had a placental clearance in rabbit that was dependent on and linearly related to the effective molecular size of the marker. Although Faber's model would predict a steeper drop in the placental permeability for larger molecules [27], in the *HRP-1* cells the observed decrease in permeability for larger molecules was substantial. The considerable decrease in  $P_e$  of the larger molecules may represent restricted diffusion as observed in the rat placenta *in vivo* for high-molecular-weight markers [30]. Qualitatively, the general profile of permeability versus effective molecular size for our *in vitro* system was in very good agreement with relationships developed for the permeation of hydrophilic substances through aqueous pores across trophoblasts constituting the rat placenta [30].

The effective molecular size of a substance is but one factor in determining the penetration of a tissue barrier by a given molecule. In this study we examined urea, methotrexate, linoleic acid, and transferrin permeation across the *HRP-1* monolayers to further establish the potential utility of the *in vitro* system in characterizing some trans-trophoblast permeation processes. Urea is believed to cross tissue barriers by both transcellular and paracellular pathways [29]. Relative to mannitol for instance, urea has a 10-fold and a 4-fold higher permeability across the syncytiotrophoblast maternal plasma membrane and basal membrane, respectively [31]. The passage of urea across *HRP-1* monolayers was greater than would be predicted solely on the basis of effective molecular size and at least three times faster than mannitol. Therefore, the enhanced permeability of urea *in vitro* might also be accounted for by both paracellular and transcellular permeation across the cells. By contrast, methotrexate has significant binding, uptake, and accumulation within trophoblasts [32]. The passage of methotrexate across *HRP-1* monolayers was substantially lower than expected based on molecular weight and might be accounted for in part by trophoblast binding and uptake which limits the availability of the drug for diffusion across the monolayers.

A critical feature of an *in vitro* system proposed as a representative model of a polarized tissue barrier is that the *in vitro* system also retains a functional asymmetry. Lafond *et al.* [33] established that linoleic acid transport by human trophoblasts was saturable, polarized, and dependent on the presence of extracellular albumin. Based on the appearance of asymmetric transport of linoleic acid in that study [33], the fatty acid was selected as a marker to test for functional asymmetry of the *HRP-1* cells. *HRP-1* cells were shown to transport linoleic acid in predominantly the apical-to-basolateral direction consistent with the observations of Lafond *et al.* [33]. Our observation affirms that,

at least with respect to linoleic acid, *HRP-1* monolayers grown on permeable supports have functional asymmetry. In related studies we have also gone on to establish saturable, albumin-dependent linoleic acid transport across the *HRP-1* cell line that was inhibited by excess unlabeled fatty acid (X. Zhang, F. Liu, M. J. Soares, and K. L. Audus, unpublished results).

Transferrin has been shown to cross human trophoblasts by an apparent transcytotic mechanism in a choriocarcinoma-derived cell line [34, 35] and by endocytosis on both apical and basolateral surfaces of normal trophoblast cultures [36]. In the rat, transferrin uptake has been shown to occur through the typical transferrin endocytic process [37]. Since, previous works had demonstrated the presence of functional transferrin receptors on the *HRP-1* cells [13, 14], we investigated the possibility that the *HRP-1* cells retain a similar apparent transferrin uptake system. We were able to demonstrate that transferrin passage across the *HRP-1* monolayer system was greater than that predicted on the basis of its molecular size. In addition, the passage of transferrin across the monolayers was concentration-dependent, saturable, bidirectional, and inhibited by unlabeled transferrin. These properties were consistent with the concentration dependence of functional transferrin receptors on the *HRP-1* cells [13, 14] and the observations for apparent transferrin transcytosis in human trophoblast cultures [34–36] and endocytosis in rat trophoblast cultures [37]. Although results here and work with the BeWo cell system have suggested transcytosis of transferrin [34, 35], *in vivo* observations have generally presupposed that transplacental transfer does not occur [38]. However, in the rat, evidence suggests that in early pregnancy maternal transferrin may be the primary source of fetal transferrin [39] and that later in gestation, cells within the placenta itself may serve as an extrahepatic source of transferrin [40]. While *in vitro* studies [34, 35] including our own suggest transtrophoblast passage of transferrin, the precise processing of transferrin by trophoblasts requires further study.

Our results suggest that the *HRP-1* cell line should have potential applications in the study of certain trophoblast transport and metabolism processes. Clearly, the cell system will have to be validated for intended applications in the study of a specific trophoblast transport system. Exploiting *HRP-1* and other monolayer-forming cell lines (e.g., BeWo) in the study of the transport and metabolism of therapeutic agents and drugs of abuse could contribute new and more detailed insights into trophoblast processes regulating the distribution of substances between maternal and fetal compartments. Since the *HRP-1* cells do undergo differentiation in the presence of an appropriate stimulus [41], this system could provide an *in vitro* system with which to study placental transport and metabolism during

the process of trophoblast differentiation. Generally, the development of tissue culture systems presents the opportunity to evaluate cellular-, biochemical-, and molecular-level mechanisms in the transport and metabolism of therapeutic agents and drugs of abuse at inaccessible tissue barriers. The advantages of such *in vitro* systems include the capacity for screening large numbers of newly synthesized agents, the requirement for minimal amounts of material, and a reduction in the numbers of costly and possibly controversial animal studies [42]. Therefore, the availability of appropriate *in vitro* trophoblast systems that might also be used to test proposed strategies in which, for example, newly synthesized therapeutic agents might be effectively inactivated to prevent crossing of the placental barrier [43] is particularly important in the development and design of agents directed toward maternal-only therapy and limiting unnecessary fetal exposure.

This research was supported by NIDA N01DA-4-7405. The authors also gratefully acknowledge the support of Corning Costar Corp. for the Cellular and Molecular Biopharmaceutics Handling Laboratory.

## REFERENCES

1. Ala-Kokko, T. I., Vahakangas, K., and Pelkonen, O. (1993) *Acta Anaesthesiol. Scand.* **37**, 47–49.
2. Enders, A. G. (1965) *Am. J. Anat.* **116**, 29–68.
3. Sibley, C. P. (1994) *Placenta* **15**, 675–691.
4. Aoki, A., Metz, J., and Forssmann, W. G. (1978) *Cell Tissue Res.* **192**, 409–422.
5. Metz, J., Heinrich, D., and Forssmann, W. G. (1976) *Anat. Anatom. Embryol.* **149**, 123–148.
6. Metz, J., Aoki, A., and Forssmann, W. G. (1978) *Cell Tissue Res.* **192**, 391–407.
7. Jones, C. J. P., and Fox, H. (1976) *J. Pathol.* **118**, 143–151.
8. Glazier, J. D., Jones, C. J. P., and Sibley, C. P. (1990) *Placenta* **11**, 451–463.
9. Matsubara, S., Tamada, T., Sayama, M., and Saito, T. (1993) *Asia Ocean. J. Obstet. Gynaecol.* **19**, 441–447.
10. Hunt, J. S., Suzuki, Y., Wood, G. W., and Soares, M. J. (1988) *Placenta* **9**, 147–158.
11. Hunt, J. S., Deb, S., Faria, T. N., Wheaton, D., and Soares, M. J. (1989) *Placenta* **10**, 161–177.
12. Soares, M. J., Schaberg, K. D., Pinal, C. S., De, S. K., Bhatia, P., and Andrews, G. K. (1987) *Dev. Biol.* **124**, 134–144.
13. Hunt, J. S., and Soares, M. J. (1988) *Placenta* **9**, 159–171.
14. De, M., Hunt, J. S., and Soares, M. J. (1988) *Biol. Reprod.* **38**, 1123–1128.
15. Laemmli, U. D. (1970) *Nature* **227**, 680–685.
16. Dutton, D. R., and Parkinson, A. R. (1989) *Arch. Biochem. Biophys.* **268**, 617–629.
17. Shiverick, K. T., Swanson, C., Salhab, A. S., and James, M. O. (1986) *J. Pharmacol. Exp. Ther.* **238**, 1108–1113.
18. Donato, M. T., Castell, J. V., and Gomez-Lechon, M. J. (1995) *Drug Metab. Disp.* **23**, 553–558.
19. Shi, F., and Audus, K. L. (1994) *Neurochem. Res.* **19**, 427–433.
20. Skidgel, R. A., and Erdos, E. G. (1984) *in Methods of Enzymatic*

- Analysis (Bergmeyer, H. U., Ed.), Vol. 5, pp. 60–72, Verlag Chemie, Weinheim.
21. Adson, T., Burton, P. S., Raub, T. J., Barsuhn, C. L., Audus, K. L., and Ho, N. F. H. (1995) *J. Pharm. Sci.* **84**, 1197–1204.
  22. Das, U., Sadiq, H. F., Soares, M. J., Hays, W. W., and Devaskar, S. U. (1996) submitted for publication.
  23. Ringler, G. E., and Strauss, J. F. (1990) *Endocr. Rev.* **11**, 105–123.
  24. Pasanen, M., and Pelkonen, O. (1994) *Crit. Rev. Toxicol.* **24**, 211–229.
  25. Pasanen, M., and Pelkonen, O. (1990) *Placenta* **11**, 75–85.
  26. Johnson, A. R., Skidgel, R. A., Gafford, J. T., and Erdos, E. G. (1984) *Peptides* **5**, 789–796.
  27. Faber, J. J. (1993) *Am. J. Physiol.* **265**, H1804–H1808.
  28. Faber, J. J., and Thornburg, K. L. (1983) *Placental Physiology*, Raven Press, New York.
  29. Stulc, J. (1989) *Placenta* **10**, 113–119.
  30. Robinson, N. R., Atkinson, D. E., Jones, C. J. P., and Sibley, C. P. (1988) *Placenta* **9**, 361–372.
  31. Jansson, T., Powell, T. L., and Illsley, N. P. (1993) *Physiology* **468**, 261–274.
  32. Sweiry, J. H., and Yudilevich, D. L. (1985) *Biochim. Biophys. Acta* **821**, 497–501.
  33. Lafond, J., Simoneau, L., Savard, R., and Gagnon, M.-C. (1994) *Eur. J. Biochem.* **226**, 707–713.
  34. Cerneus, D. P., and van der Ende, A. (1991) *J. Cell Biol.* **114**, 1149–1158.
  35. Cerneus, D. P., Strous, G. J., and van der Ende, A. (1993) *J. Cell Biol.* **122**, 1223–1230.
  36. Verrijt, C. E. H., Cleton-Soeteman, M. I., Kroos, M. J., and van Dijk, J. P. (1996) *Placenta* **17**, A.34.
  37. McArdle, H. J., Douglas, A. J., and Morgan, E. H. (1985) *J. Cell Physiol.* **122**, 405–409.
  38. Contractor, S. F., and Eaton, B. M. (1986) *Cell Biochem. Funct.* **4**, 69–74.
  39. Huxham, I. M., and Beck, F. (1985) *Dev. Biol.* **110**, 75–83.
  40. Boockfor, F. R., Harris, S. E., Barto, J. M., and Bonner, J. M. (1994) *Placenta* **15**, 501–509.
  41. Soares, M. J., De, M., Pinal, C. S., and Hunt, J. S. (1989) *Biol. Reprod.* **40**, 435–447.
  42. Audus, K. L., Bartel, R. L., Hidalgo, I. J., and Borchardt, R. T. (1990) *Pharm. Res.* **7**, 435–451.
  43. Rapaka, R. S., and Porreca, F. (1991) *Pharm. Res.* **8**, 1–8.

Received January 6, 1997

Revised version received March 24, 1997